

**PHASE I FINAL REPORT
NDI METHOD FOR QUANTIFICATION OF WEAK
BONDING STRENGTH OF COMPOSITE STRUCTURES**

R. F. Johnson

August 1997

Prepared for
U.S. NAVY
Under Contract No. N00189-96-M-JT09



QUEST INTEGRATED, INC.
21414 - 68th Avenue South
Kent, Washington 98032
(206) 872-9500

19990421 020

DISTRIBUTION STATEMENT A
Approved for Public Release
Distribution Unlimited

**PHASE I FINAL REPORT
NDI METHOD FOR QUANTIFICATION OF WEAK
BONDING STRENGTH OF COMPOSITE STRUCTURES**

R. F. Johnson

August 1997

Prepared for
U.S. NAVY
Under Contract No. N00189-96-M-JT09

**Approved for Public Release;
Distribution Unlimited**



QUEST INTEGRATED, INC.

21414 - 68th Avenue South
Kent, Washington 98032
(253) 872-9500

TABLE OF CONTENTS

INTRODUCTION	1
RESEARCH PLAN	1
SHEAROGRAM LAB AND IMAGE ACQUISITION	2
Brief Review Of Shearography	2
Shearography vs. Holography	2
Synchronous Shearography	3
Shearography Laboratory	4
FINITE ELEMENT ANALYSIS (FEA) MODELING OF COMPOSITE PANELS	6
MANUFACTURE OF PANELS	11
TESTING THE PANELS	11
Thermal Excitation Testing	12
Microwave Excitation Testing	12
SHEAROGRAPHY LAB TESTING OF PANELS	13
Relative Ranking - Coin Drop Frequency Test Results	19
Destructive Testing	20
Calibration	20
Field System	22
CONCLUSIONS	23

INTRODUCTION

This Phase I Final Report is for a Small Business Innovation Research program conducted for the Navy under Federal Contract N00189-96-M-JT09. The purpose was to investigate ways to determine the overall strength of a composite structure by using a nondestructive evaluative (NDE) optical technique, shearography. The purpose of the research was to determine if there is an effective way to assess the strength of composite components on in-service aircraft rather than in the front end of the composite manufacturing process. The goal was to determine the overall feasibility of such an NDE method, and to investigate various means of probing the material under test.

The work involved analyzing how a composite structure behaves under thermal and acoustic excitation, and then trying to reproduce the results on actual shearography hardware and verify the same behavior on laboratory specimens. The comparisons are made with respect to a constructed FEA model of epoxy/carbon composite panel. The panels were "built" in different ways to simulate the overall weakening of a composite component. This is different than using shearography to examine a component for localized defects. In searching for localized defects, the defects appear as unique fingerprints that can usually be easily discerned from the background fringe pattern. In looking for an overall weak component, the research took the approach that a weak component is going to assume a different shape under acoustic or thermal excitation than a strong one. Specifically, the frequency of vibration of a weak component will be lower for a given fundamental mode of vibration than a component that has normal flexural strength. A synchronization circuit enables the capturing of images at their peak amplitude, thereby reducing blurring due to decorrelation of speckle.

RESEARCH PLAN

The purpose of this research was to show if there is a relationship between the overall strength of a composite panel and its shear stiffness. The stiffness of a composite would be measured nondestructively using optical shearography. Shearography is a sensitive method for measuring the shape of a surface based on its observed fringe pattern. The hypothesis is that generally overall weak composite specimens will vibrate at lower frequencies under acoustic excitation than strong composites. The motivation of the customer was to determine specifically if the overall weakness of a composite structure could be learned by a shearography technique. The ability to detect disbonds has been demonstrated previously in commercial hardware (Laser Technology, Inc. and others) and in the laboratory by QUEST, and was considered to be new work. It is a much more difficult problem to determine in a reliable manner if a component has lost strength due to long term water absorption (carrier based aircraft), the accumulation of many microcracks (fatigue cycles) or an improper field repair to a composite portion of an aircraft (poor manufacturing). The focus of this effort was to learn how different excitation methods could reveal an overall weak component.

The overall research included:

- Assembly of a temporary shearogram lab;
- FEA (finite element analysis) of how panel sections behave under excitation
- The manufacture of composite test panels
- Testing the panels in the shearing lab

- Destructively testing the panels for strength
- Comparing shearography results with the destructive testing

Each of these tasks is more fully explained in the following sections.

SHEAROGRAPH LAB AND IMAGE ACQUISITION

Brief Review Of Shearography

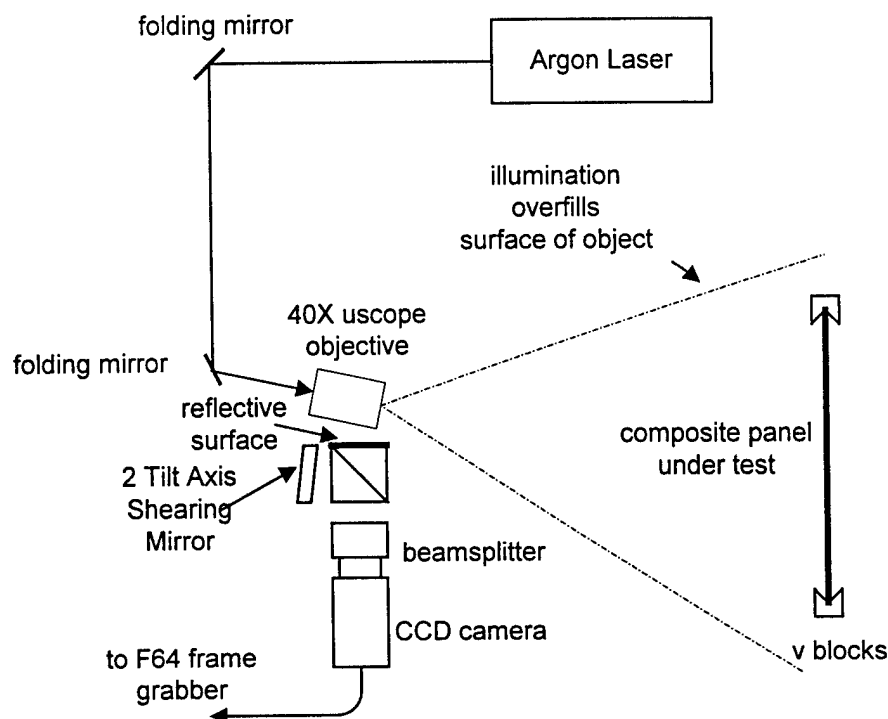
Shearography was originally developed for measuring strains in materials. It is an interferometric method which allows for wide field measurement of surface displacement derivatives. The surface to be examined is illuminated with an expanded beam from a laser. The object is imaged with an image shearing lens system onto film or a CCD (charge coupled device) video imaging array. The image shearing lens system consists, in its simplest form, of a thin, weak wedge prism covering one half of a conventional lens. This combination of lens and prism produce two equally bright, laterally displaced images. These displaced, or "sheared" images are formed when light from two different points on the surface of interest are brought into focus in a common point on the film or detector plane. The distance between the two points on the surface under test is called the shearing distance. Because laser light is coherent, the sheared image is a vast, random interference map commonly called a speckle pattern. When the object is slightly disturbed, this speckle pattern is modified. The superposition of two speckle patterns resulting from a double exposure of a surface in the undeformed and deformed state yields a fringe pattern. This fringe pattern is a gradient map of the surface displacement field. The amount of sensitivity of the measurement of the gradient of the surface is proportional to the shearing distance.

Shearography vs. Holography

As was described before, shearography measures the stain of a surface whereas holography measures the normal displacement of the surface. Local defects create strain concentrations and it is easier to detect and visualize strain patterns than displacement patterns. Since shearography measures displacement gradients, it is not sensitive to rigid body motion. In holography, rigid body motions create uninterpretable images and confusing fringe patterns. Shearing systems are easy to set up and have simpler optics than holography. It relaxes the vibration isolation requirements and is thus more suited to field applications. The coherence length requirements are substantially reduced, leading to systems being constructed using compact laser diodes, rather than expensive and cumbersome ion lasers. A huge benefit is the controllable range of sensitivity by changing the shearing distance by adjusting the wedge angle of the prism or the mirror; whichever optical element is used. Finally, the resolution of the recording media is greatly reduced, allowing for less expensive photographic and video recording of fringe patterns.

Figure 1 depicts the generic shearography apparatus used for this Phase I research. It consists of relatively simple hardware. Instead of the wedge prism described previously, the more practical approach is shown here; a cube beamsplitter with one silvered face and a two axis adjustable mirror. The 50 mm beamsplitter is a non-polarized 50%/50% type. The beamsplitter face opposite the camera is fully aluminized. The light from the scene is reflected at the hypotenuse of the beamsplitter and on to either the aluminized face or the adjustable mirror. It is reflected again at the hypotenuse for light reflected from

the adjustable mirror; it is transmitted at the hypotenuse for light reflected from the aluminized face. By slightly tilting the mirror any amount of shearing distance can be produced at the object surface.



SHEAROGRAPHY of COMPOSITES Optical Components

Figure 1. Shearing Optics

The laser used for the source was an argon ion type running at a single wavelength of 514 nm and at a continuous wave power of 1 W. The raw beam from the laser is folded using several adjustable mirrors and is then directed into a 40X microscope objective. This forms the laser beam into a large cone which is then directed to the surface of the object; overfilling it. The angle of incidence of the laser light on the surface of the object affects the slope sensitivity; these geometric constants are either calculated from the set up, or can be determined by varying the slope of an object in the illumination field by a known amount. (See Calibration)

Synchronous Shearography

In synchronous shearography the contrast of a shearogram can be increased by electronically locking the frame capture time of the CCD camera to the same point on the repetitive portion of the excitation cycle. Usually the excitation type that is best suited for this is vacuum or acoustic; heating excitation is too slow and not at all periodic nor particularly reproducible. This synchronous technique reduces the decorrelation noise of a typical shearing image because it acts as a strobe light does in conventional photography.

Shearography Laboratory

A special lab was set up for this research. A 5W (all wavelengths) argon-ion laser, (Spectra Physics Model 164 Argon Ion Laser), shearing optics and reference mirrors, the camera (Cohu Model 8400, a full frame transfer CCD camera) and the part fixture all are situated on a 4' x 4' x 2 inch thick honeycomb optical table. A '486 computer with a frame grabber board Coreco F64 data acquisition board) and attached DSP (digital signal processor) allowed for real time image processing of video signals from the CCD camera. The DSP allowed for 250 million floating point operations per second. This allows image subtraction required for the revealing the shearing fringes to be performed in real-time. It also lets other functions be performed such as edge enhancement filters, histogram compensation, high and low pass filters and Laplacian filters. A photo of the lab is shown in Figure 2.

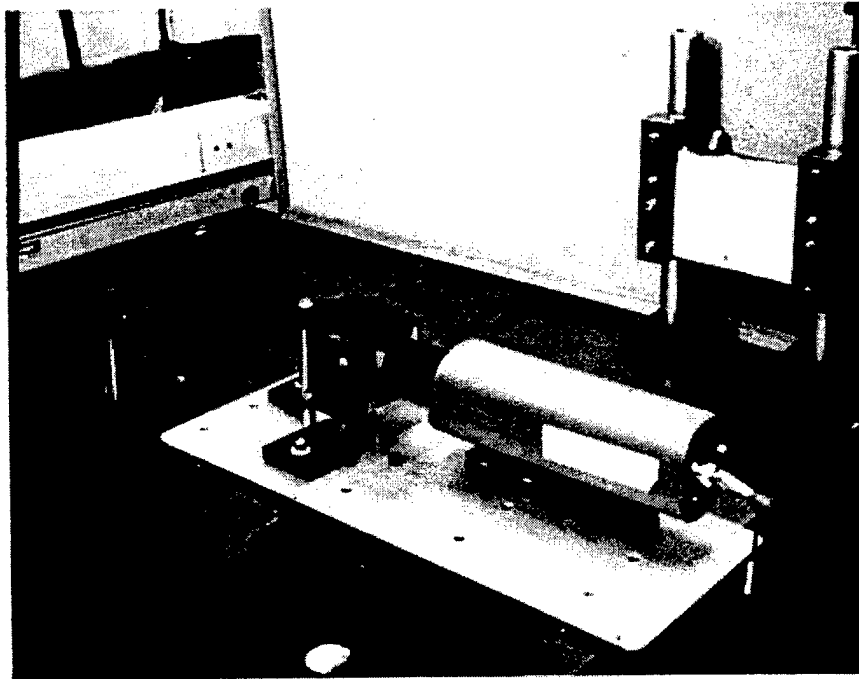


Figure 2. Shearography Test Station

The laboratory apparatus used in this research is listed below:

- Dell '486 computer, 66 MHz, 16 Mbytes of RAM
- Spectra Physics Model 164 Argon Ion Laser
- Cohu Model 8400 full frame transfer CCD camera
- Coreco F64 Data Acquisition Board
- JBL 2445 Compression Driver; 2 to 20 kHz
- JBL 2385 60 degree Horn
- QSC MX700 200W Audio Amplifier
- TDM 24CX2 Crossover Network
- Wavetek 1410 Audio Oscillator

- Melles Griot 03 BSC 015 hybrid beamsplitter; 50 mm cube
- Melles Griot 02 MFG 005 plane mirrors; 50 mm square
- Melles Griot 04 OAS 016 40X microscope objective
- Newport 4 ft. by 4ft. optical table

The electronics portion of the shearing lab consisted of a '486 personal computer, the acoustic source and amplifier, the synchronization circuit, and the CCD camera and frame grabber board which resides inside the personal computer. To acquire a shearogram on a normal object whose shape changed slowly due to thermal effects the two step procedure was to use what is known as image subtraction, or change detection. A simple and powerful method, it has found wide use in analysis of medical images and in industry for inspecting missing parts on circuit boards. It consists of aligning two images and then subtracting them on a pixel by pixel basis. If the two scene are the same, the result is a totally black image. Any changes show up as gray scale patches.

1. Acquire and store a REFERENCE gray scale image
2. SUBTRACT the REFERENCE from subsequent camera images

An amplified explanation follows. The CCD camera is connected to a frame grabber and buffer. When the computer is told to store the image, the entire image of 1024 x 780 pixels is stored in RAM (random access memory). This image is three dimensional, in that each pixel location has associated with it an 8 bit byte representing brightness; a 0 represents black and a value of 255 represents white. Mathematically, the stored reference image is represented as:

Eqn. 1

$$r(x, y) = \sum_{m=0}^{1023} \sum_{n=0}^{779} I\left(\frac{\Delta x m}{1023}\right) I\left(\frac{\Delta y n}{779}\right)$$

The summation signs described the image sampling process. The $I(\)$'s represent the intensity of each sampled point in the image. For simplicity, subsequent representation of the images will be indicated by the simpler left hand side of the equation. It is understood that the image is decimated and stored by the frame grabber, that it is a two dimensional image where an intensity value at each x_m and y_n point can have a value ranging from 0 to 255.

The subtraction process consists of following image processing step:

Eqn. 2

$$s_i(x, y) = u_i(x, y) - r_{i-1}(x, y)$$

where $i = 1, 2, \dots$

The result of the subtraction process is $s(x, y)$ which is displayed in real time, and where any value less than zero are displayed as a 0.

This is accomplished with a frame grabber and image processor if the image is not changing too rapidly. For example, thermal effects occurred slowly and a simple storage of the reference image and the image of the object under test were displaced in time by tens of seconds. To do the same task in a shearography system with acoustic excitation the capabilities of real-time image processing hardware. The F64 board

with its collocated image processor capable of 250 million floating point operations per second was chosen for this reason.

The acoustic excitation testing of panels proceeded two ways; shearography via standing wave image acquisition and acoustic synchronization of images. Standing wave methods involved using the reference image of an unexcited panel

FINITE ELEMENT ANALYSIS (FEA) MODELING OF COMPOSITE PANELS

A comprehensive model was made of two sandwiched panels made of carbon composite and a resin matrix. Each panel consisted of plies laid in a 0-90-0 orientation. A three dimensional models was built and tested, and then a two dimension model was constructed. The 2D model ran much more quickly and gave just a good results because of the thin nature of the panel. For thermal excitation sources, heat was allowed to soak in from one side of the part and the shape change recorded; for microwave excitation the part was uniformly heated. For the vibration method, the acoustic source consisted of a plane wave launched at the panel from one side. For both the thermal and acoustic excitation method, the modeled panel had dimensions of 12 inches long by 6 inches wide by 0.25 inches thick. The panel was fixed on its two short sides and allowed to rotate; the 6 inch sides were fixed in v grooves and rotation along that was performed.

The weak bond was modeled two ways:

1. An epoxy bond layer which has a uniformly smaller shear stiffness modulus but is otherwise in perfect adhesion to both panels.
2. An epoxy bond layer whose shear stiffness is the usual value, but has a checkerboard bonding pattern. A certain percentage of the checkerboard elements are not bonded, i.e. where a bond of zero strength exists between the two panels.

In the first case the "strength" can be varied by changing the effective shear modulus. In the second case, the strength is varied by changing the number of epoxy elements which are actually bonded to the plates. This requires more careful FE construction so that "bonded" elements share nodes while "unbonded" do not share nodes on the interface. The software used to output the graphical results functions as a pre and post processor. This software, FEMAP, also is used to build the grids, apply boundary conditions and apply loads. The actual analysis software used is called ABACUS.

For the good bond geometry, the steps are:

- Build geometry
- ABAQUS run with n different stiffness

For weak bond as patchwork of unbonded elements, the steps are:

- Build geometry with n different bonds
- ABACUS run with n different bonds

For the overall weak board:

- Build geometry (essentially the same as the strong, normal bond strength)
- ABACUS run with weak bonds

Once the panels were manufactured and the as-built dimensions were known, the FEA models were dimension adjusted to reflect the dimensions of the parts. Then the model was allow to run for each of the three models. It was programmed to detect only a certain set of modes. The mode condition was:

Eqn. 3
$$2L/\lambda = m;$$

where λ is the wavelength and L is the length(width) of the panel in the X(Y) axis; allowing , only integer half waves in the X and Y axes.

When the program found a example of the mode criterion it logged the acoustic excitation frequency which excite the mode. What was unknown was what the mode looked like. After a mode run of the first 20 modes, which took days of computer time, the modes were graphed. Only the set of modes which had variations in amplitude along the X axis were to be use, as these were the easiest modes to reproduce in the laboratory. Other modes where there are variations in amplitudes in both axes are difficult to reproduce. The V-blocks placed such a restriction on the boundary conditions that searching only for modes in which there were variations along the X axis but none in the Y axis met the requirements.

Finally, to match the most efficient portion of the acoustic driver's output of 1 to 4 kHz with the manufactured boards, it was decided to investigate the 3rd and 4th harmonic along the X axis. Thus the testing was to explore the cases where the panel vibrates with three half waves along the X axis and with 4 half waves along the axis. Again, there was to be no variation at all along the Y axis, and the v-blocks were to assure this. The modes which represented the 3rd and 4th harmonics were number 7 and 11, respectively. Modes 1, 3, 7, 11 and 18 were the modes which only had variations in amplitude along the X axis. Mode 1 is the fundamental mode of vibration. It was checked against that of a simple, uniform beam and was found to agree to with 2% in frequency, and so the FEA method of analyzing modal vibrations was deemed to give good results.

Figure 3 depicts two sets of graphs of for the first 20 modes. The top half of the figure plots the modes for a panel thickness of 0.125 inches, and another set of modes for the as built 0.1045 inch thickness. As the mode number increases, there is a larger frequency difference for the same modal shape. For example, mode 11 for the 0.125 inch thick panels indicates a frequency of 2772 Hz, and for the 0.1045 inch thick panel it is only 2350. This behavior represents a modals frequency which is proportional to the thickness of the panel.

For the weaker bonded panels the results present less of a means to extract flexural strength based on frequency. In the lower portions of Figure 3 are graphed the modal frequency for the normal strong panel with a thickness of 0.125 inches, the 10% overall weak panel, and a panel made of a checkerboard patchwork of normal bonds. It was unknown how to model the generally weak composite structure, so two avenues were taken. One was to model the strong panel with an overall reduction in shear modulus of 10%. The other way was to assume normal bonding between the two panels, but in only 10% of area. The grid size for the patchwork or checkerboard pattern was 0.5 inches on a side.

The FEA bending results of the panels are graphed in Figures 4 and 5 below for modes, 1, 3 7, 11 and 18. The shape is identical for the strong and overall weak structure but the frequency slightly different. The shape of the modes is different for the checkerboard pattern of normal bonds.

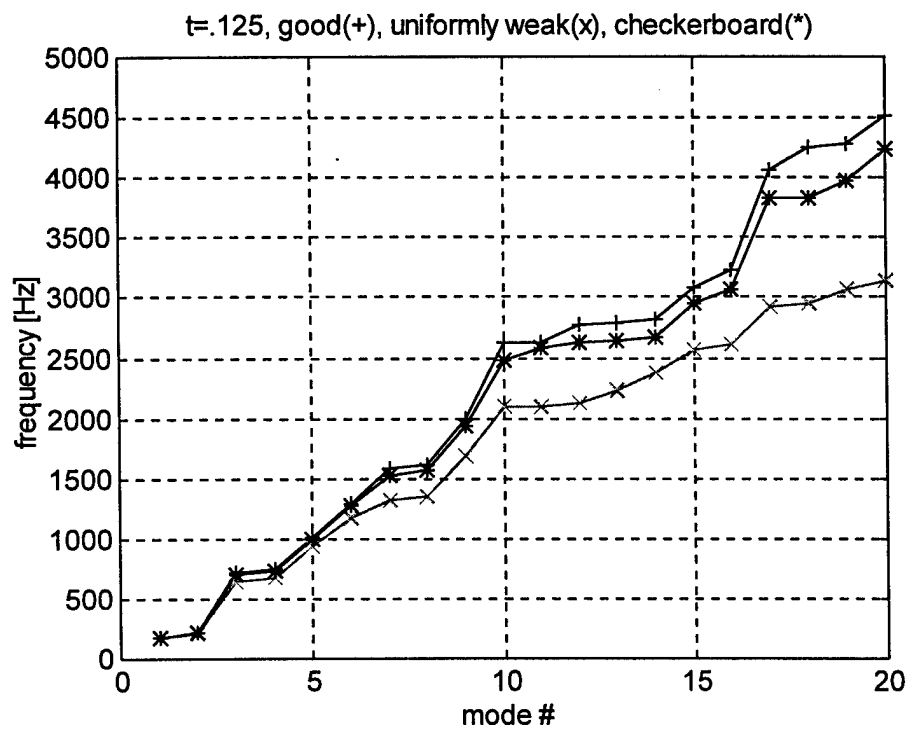
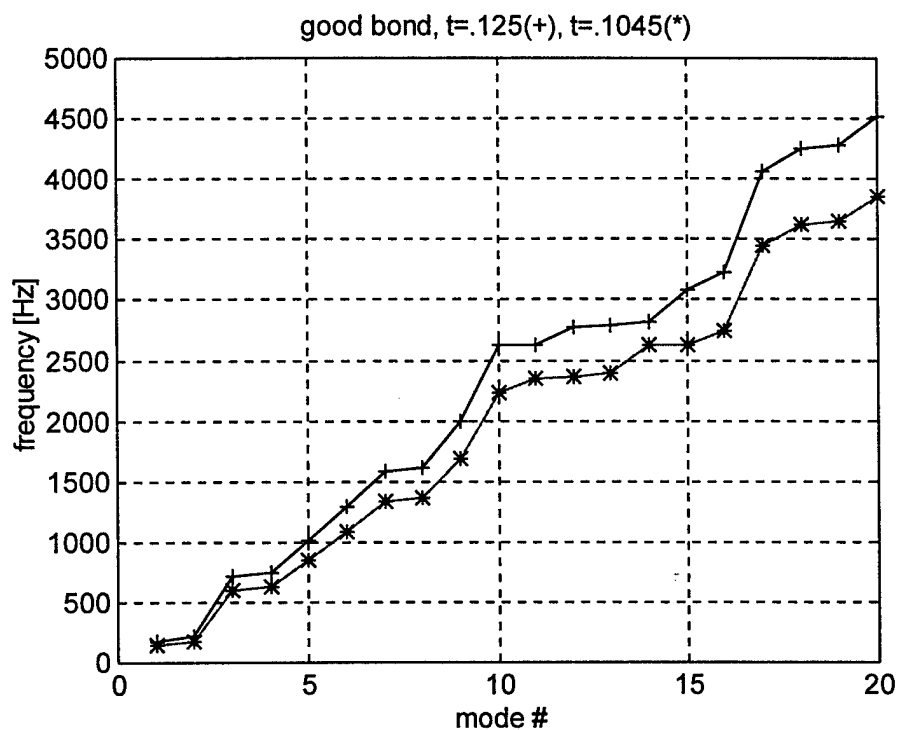
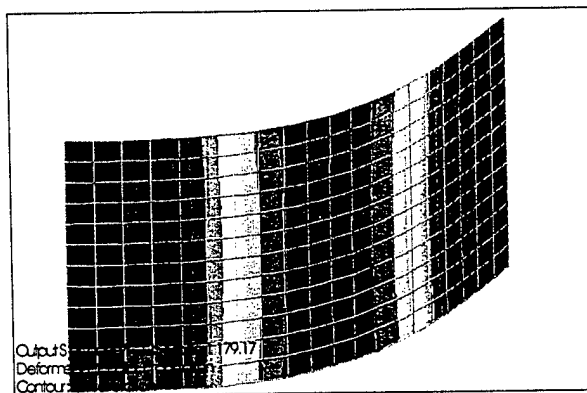
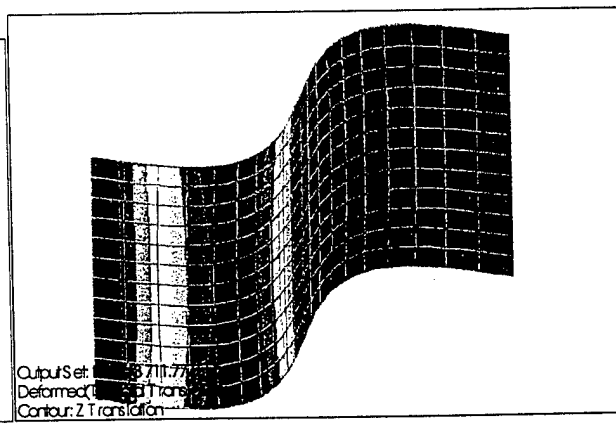


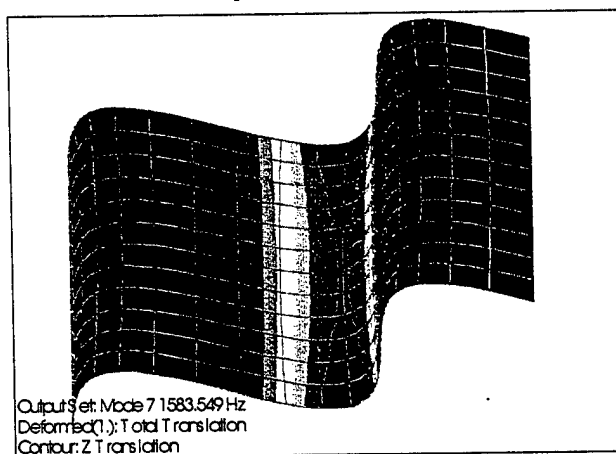
Figure 3. FEA Results for First 20 Vibration Modes



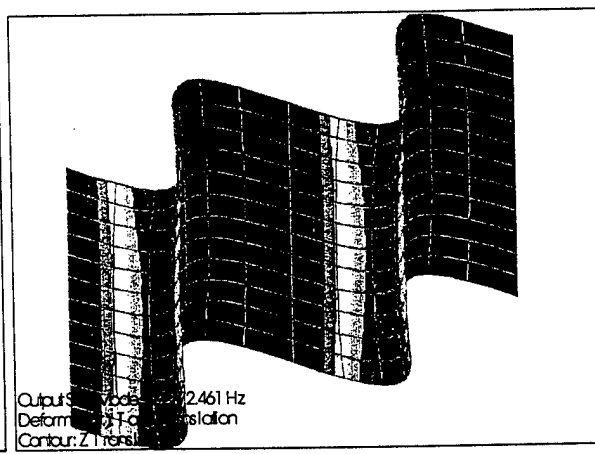
$f_1 = 179\text{Hz}$



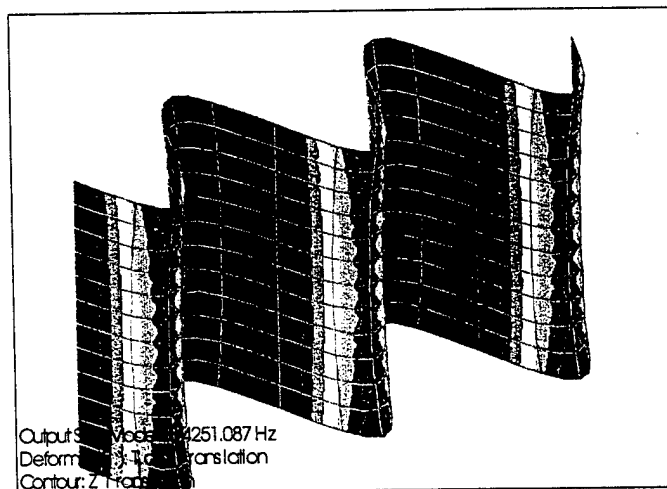
$f_3 = 711\text{Hz}$



$f_7 = 1583\text{Hz}$

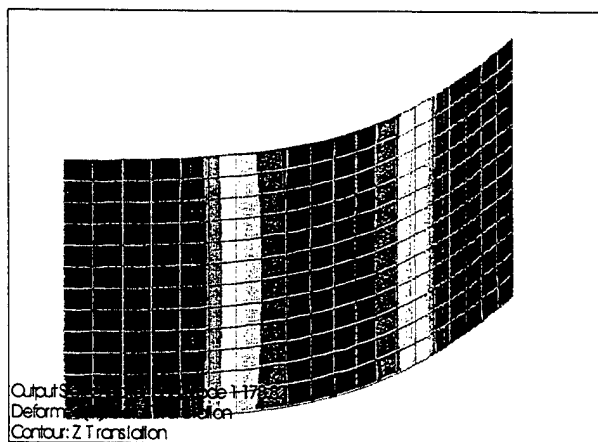


$f_{11} = 2772\text{Hz}$

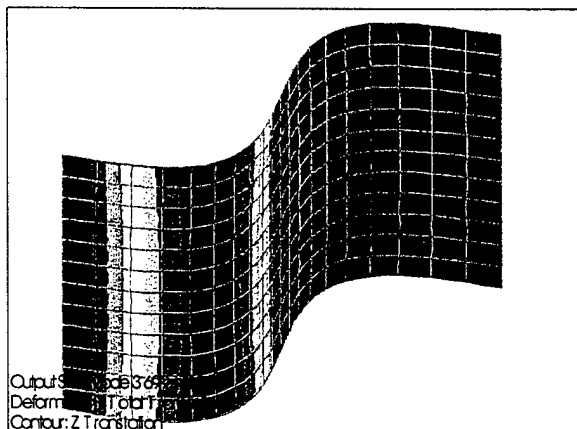


$f_{18} = 4251\text{Hz}$

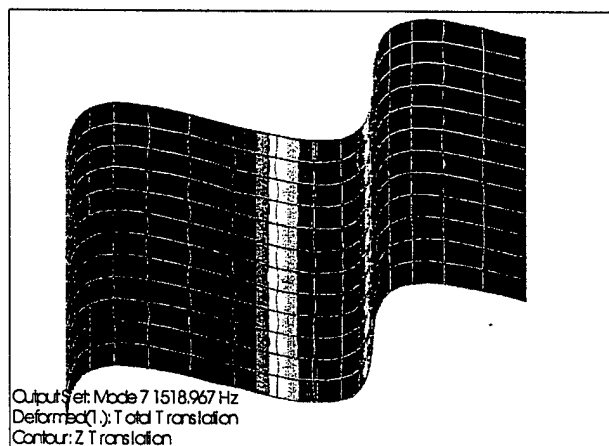
Figure 4. FEA Shapes of Modes 1,3,11, and 18 for Strong and Overall Weak Bonds



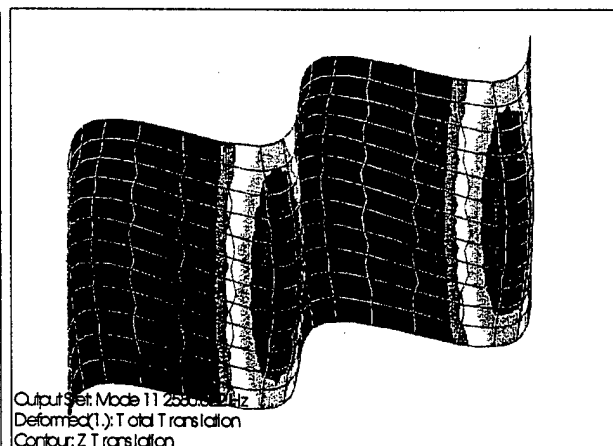
$f_1 = 179\text{Hz}$



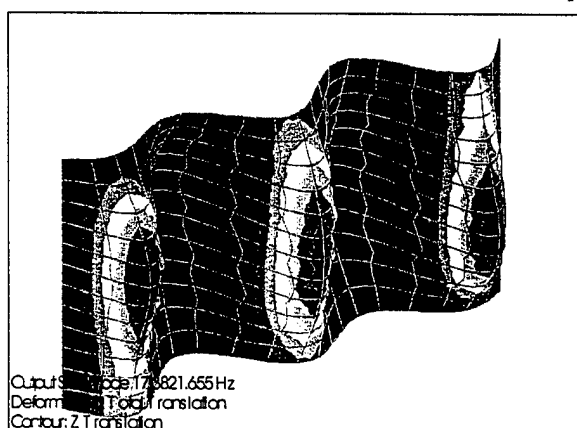
$f_3 = 699\text{Hz}$



$f_7 = 1519\text{Hz}$



$f_{11} = 2580\text{Hz}$



$f_{17} = 3821\text{Hz}$

Figure 5. FEA Shapes of Modes 1,3,11, and 18 for Checkerboard Weak Bonds

The discouraging part of the results is that the frequency difference between the normal and the checkerboard bonds is small. In no case did the model suggest there was a higher modal frequency, but the difference for a 10% weak structure and the 100% strong structure was only 50 Hz. At mode 18 it was better, a 420 Hz difference. For the overall weak panel and the normal panel the difference as larger; 200 Hz at mode 7 and 500 Hz at mode 11. Only lab testing would reveal the nature of the modeled bonding

MANUFACTURE OF PANELS

The three panels were manufactured by Dr. Sue Mantell of the Mechanical Engineering Dept. of the University of Minnesota. The carbon fibers used are Fiberite 977-3, uniaxially laid, and bound with a toughened epoxy matrix. The tensile strength of the fibers in a 0 degree orientation is 364 KSI and 9.3 KSI with the fibers oriented at 90 degrees. The control sample was made by consolidating 8 layers of ply under a 20 inch vacuum, followed by a 6 hour post cure in an autoclave at 350 degrees F and 80 PSI pressure. The 90% strength sample was made by reducing the cure time to 2 and 3 hours, respectively. All other parameters remained the same. The weak panel was made using the same curing times and pressures, but the two subpanels each had many areas of Teflon film inserted prior to consolidation to simulate poor contact adhesion. Each subpanel after consolidation had a thickness of 0.055 inches. Two of these sub-panels were then bonded together using 3M adhesive film FM-300. The overall thickness of the manufactured panel was 0.11 inches. The cure time and temperature of the bonding together of the two sub-panels was accounted for in the overall cure time. Dr. Mantel did not indicate the identity of the panels before experimentation and testing commenced. The only identification were identifying numbers on each panel. This allowed for blind testing and removed experimental bias.

The manufactured panel data was:

	<u>Panel #1</u>	<u>Panel #2</u>	<u>Panel #3</u>
Height	25.39 cm	25.46 cm	25.42 cm
Width	15.48 cm	15.52 cm	15.446 cm
Thickness	0.270 cm	0.265 cm	0.264 cm
Weight	155.0 gms	154.0 gms	153.5 gms
Density	1.460 g/cc	1.470 g/cc	1.481 g/cc

TESTING THE PANELS

The testing geometry was the same for all excitation tests. The panels were restrained along their short sides by a two 90 degree V-grooves made of 1 inch thick steel. Thus the boundary conditions of the panels allowed for free rotation about the axis define by the groove, but it constrained its position. This reproduced the general situation for a panel bonded to a stringer in an airframe, though the boundary conditions at a stringer are both position constrained (free rotation) and slope constrained (clamped). For a practical reason the free rotation boundary condition was used because it more closely matched the peak acoustic output range of the compression driver used. A clamped boundary condition exhibits a higher frequency of vibration for the same modal shape as the freely rotating boundary condition.

For acoustic testing, the sound was produced by a piezoelectrically driven source (JBL 2445 Compression Driver; 2 to 20 kHz) An exponential horn (JBL 2385 60 degree Horn) was connected to a 200 watt amplifier (QSC MX700 200W Amplifier); the driver was protected against overdriving it with passive components (TDM 24CX2 Crossover Network). The amplifier was driven by a variable frequency sine wave oscillator, (Wavetek 1410). The acoustic driver was situated approximately 1 foot from the panel and at normal incidence.

Thermal Excitation Testing

Heating tests consisted of using a hot air gun to generally heat the panel surface, or microwaves from a conventional oven to do the same task. The first heat source tested was a heat gun. The panel was held by its short side edges in v-grooves. The reference image was taken and stored, and then heat was applied via a heat gun. Two problems arose with this technique. First, it was difficult to get uniform heating across the surface of the part. By "painting" the hot air plume over the surface of the part in a carefully practiced manner, the part could be heated somewhat uniformly. But it was difficult to do in practice because it would take a long time, and the technician didn't know how good a job was being done in applying the heat. Second, the sensitive nature of shearography led to a "fogging" effect created by the conduction of heat from the panel to the air. This caused convection currents above the surface of the part which in turn led to optical phase shifts in the air path over time. This created a shearogram which caused visible shearing patterns consisting in most cases of random streaks and a general, low contrast image. Figure 6 shows the plume from a hot air gun 10 seconds after the heat element was turned off. Because of the difficulty in creating a uniformly heated surface and in getting any meaningful shearograms, this excitation approach was abandoned.

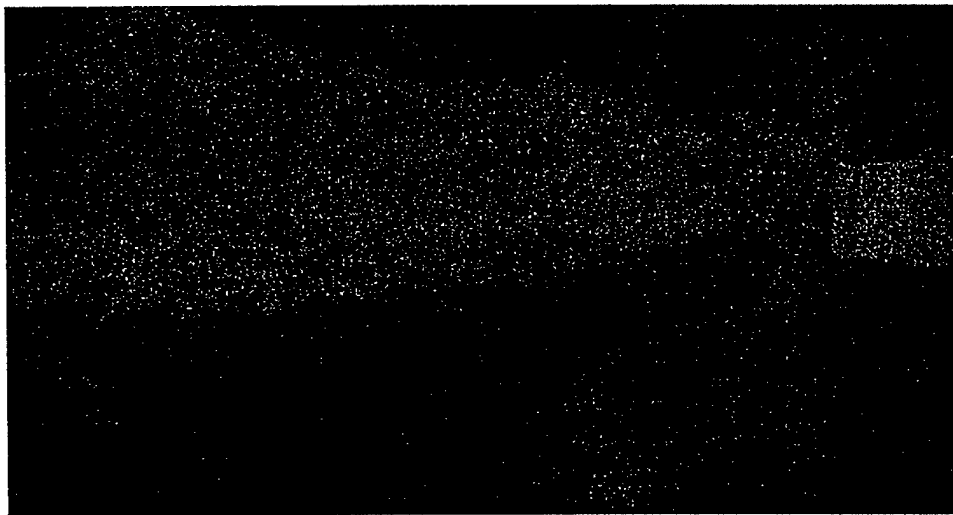


Figure 6. Shearogram of Hot Air Gun Plume 10 Seconds After Heat Element Turned Off

Microwave Excitation Testing

Thermal excitation using microwaves was done using a commercial oven with its door interlock defeated. The door to a 1500 watt oven was removed and the panel placed in the plane where the door was

formerly located. Because the panel width was narrower than the door, metal strips were placed next to the panel to reflect the microwaves back into the cavity. It was not practical to place the sample panel in the microwave cavity because the Faraday screen which protects the user for microwaves does not allow an adequate shearogram to be made. Because of the parallax required to make a shearogram, the grid being interposed between the sample and the optics lead to an obscuration and a Moire' pattern which obliterates the shearogram.

The microwaves heated the panel surface from the back. Images were not taken when the technician was present; instead the images were observed on the computer screen located around and behind a metal screen. When the desired amount of movement had occurred the image was stored. Obviously, since any thermal method is not fast in terms of frequency response, no synchronizing was needed nor done. As the surface was heated from behind, there was a general response that occurred in the following sequence: at first, the surface bowed inward to the microwave cavity, or away from the shearing optics; this effect occurred during the first 10 seconds of excitation; this was unexpected. Then as the composite panel material uniformly heated up it assumed its original shape. If the panel was situated in the v-block in such a manner that there was a lot of mechanical preload in the direction of the long axis, then the small amount of expansion due to overall heating would bow the panel either outward or inward; it could never be predicted nor controlled.

Active thermal heating via hot air and microwave excitation did not present significant amounts of useful information. There was no stable shape that could be generated with the technique. Also, general FEA modeling of the panels took more time than was expected. It was important to produce FEA models that were sufficiently accurate for laboratory purposes. Since there was only a small fixed budget for FEA design and analysis, all the FEA work was directed at modeling the results of sinusoidal acoustic excitation methods.

SHEAROGRAPHY LAB TESTING OF PANELS

The FEA modeling and analysis work was directed towards edge constrained panels under acoustic excitation from the front and normal to the surface of the part. In particular, the modal shapes of 1.5 standing waves across the surface of the part and 2 complete waves were taken as the standard to which work was directed. These are close to the fundamental frequency of vibration of the panel. However, using the lower frequency of excitation is designed to detect the overall strength of the panel and not be sensitive to local disturbances such as small regions of disbonding. A lower frequency of excitation yielding the same mode shape must only be due to an overall reduction in strength of the panel.

The FEA work was carried out for three types of bonded panel sections. The goal was to make a normal part that consisted of two 0.06 inch (nominally) thick subpanels bonded together. This simulates a typical field repair or a manufacturing situation where two components must be bonded together after each has been fabricated. The control panel was bonded according to a specification made available by Boeing. The other two were made at reduced strength. The variation in strength was done by reducing the cure time and temperature. Dr. Mantel has done much work in this area for other NDE techniques, and has gained experience on how to make poor samples at a desired reduction in flexural strength.

The three panels which were manufactured and tested were to be of the following relative strengths:

- Normal, Strongly Bonded

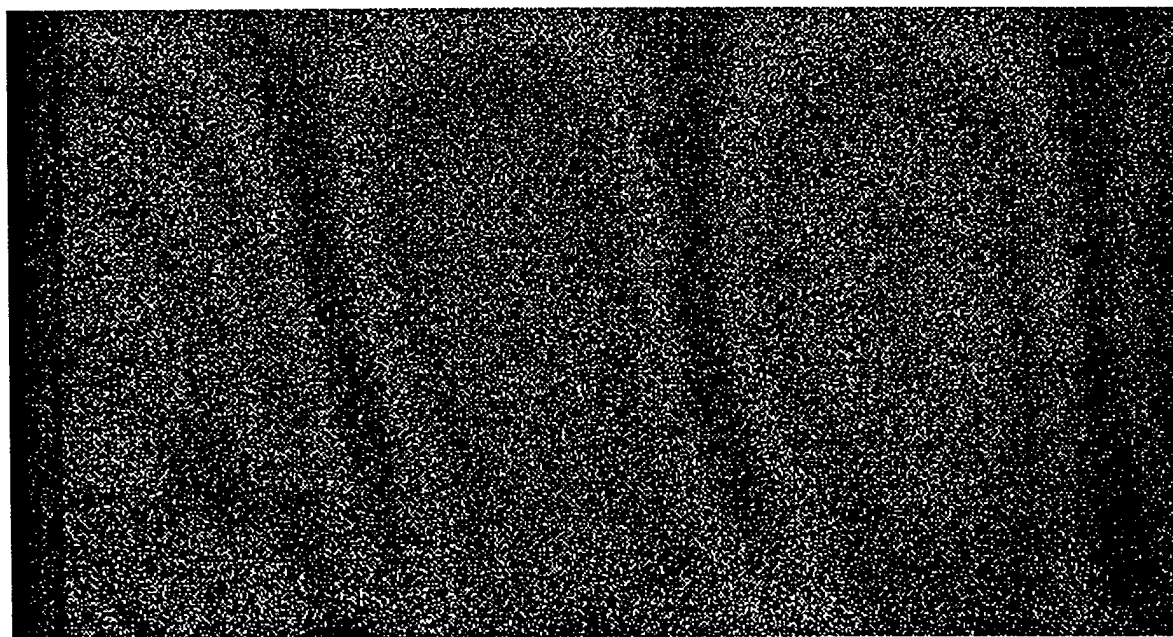
- 90% Flexural Strength
- 50% Flexural Strength

There was simply no way for Dr. Mantel to make a 10% strength panel. Although the FEA modeling work used 10% as the "weak" panel, practical experience indicated that such a panel could not be manufactured. In normal airframes, such a weakness would also never be experienced, so higher strength panels were made. Destructive testing done later would reveal the actual relative strengths of the panels.

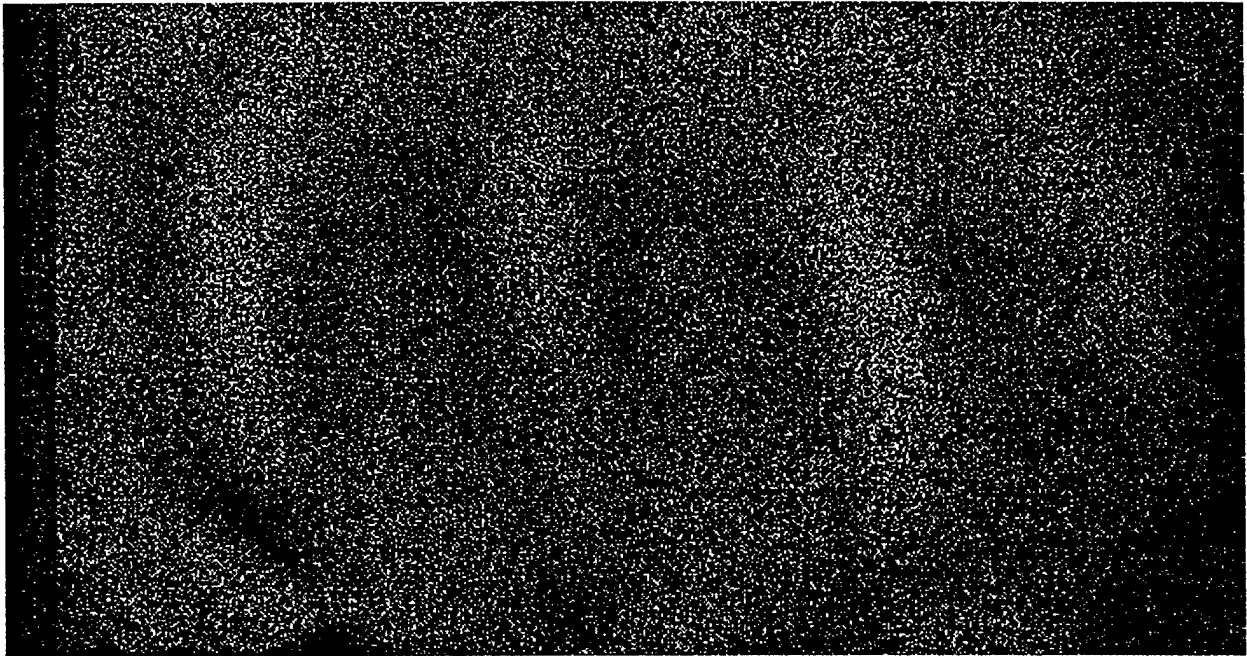
Each panel was in turn put into the test V-block fixture and approximately 20 watts of acoustic energy directed normal to surface at a distance of 2 feet. The two stable modal shapes of 1.5 and 2 complete wavelengths were gained by observation and were tuned by adjusting the frequency of the sine wave oscillator. The panels were labeled #1, #2 and #3, and during testing the strength of the panels was not known, eliminating experimental bias. Since shearography produces the gradient of the displacement field, the characteristics of the 1.5 and 2 wavelength patterns of the two patterns had three and four bands, respectively. The bands are actually areas of the shearogram where the displacement of the actual surface is at a sinewave maximum or minimum. Here the shearogram's fringe pattern is not changing rapidly with distance along the <X> axis and so shows up as a bright band.

The qualitative laboratory results are described. In the shearograms which follow, the X axis is in the vertical direction and Y runs across the page left to right. The top of the panel is the top of the shearogram. After the two harmonic shearograms is the reference image. It does not show fringes because, of course, it is the image from which the dynamic ones are subtracted. All of the images were imported into Paint Shop Pro and only modestly post processed. The processing consisted of cropping the image and adjusting the overall contrast. Each shearogram image required approximately half a megabyte of memory storage.

Panel #1 - Third Harmonic; Excitation Frequency: 1700 Hz.



Panel #1 - Fourth Harmonic; Excitation Frequency: 2800 Hz.



Reference Image of Panel #1

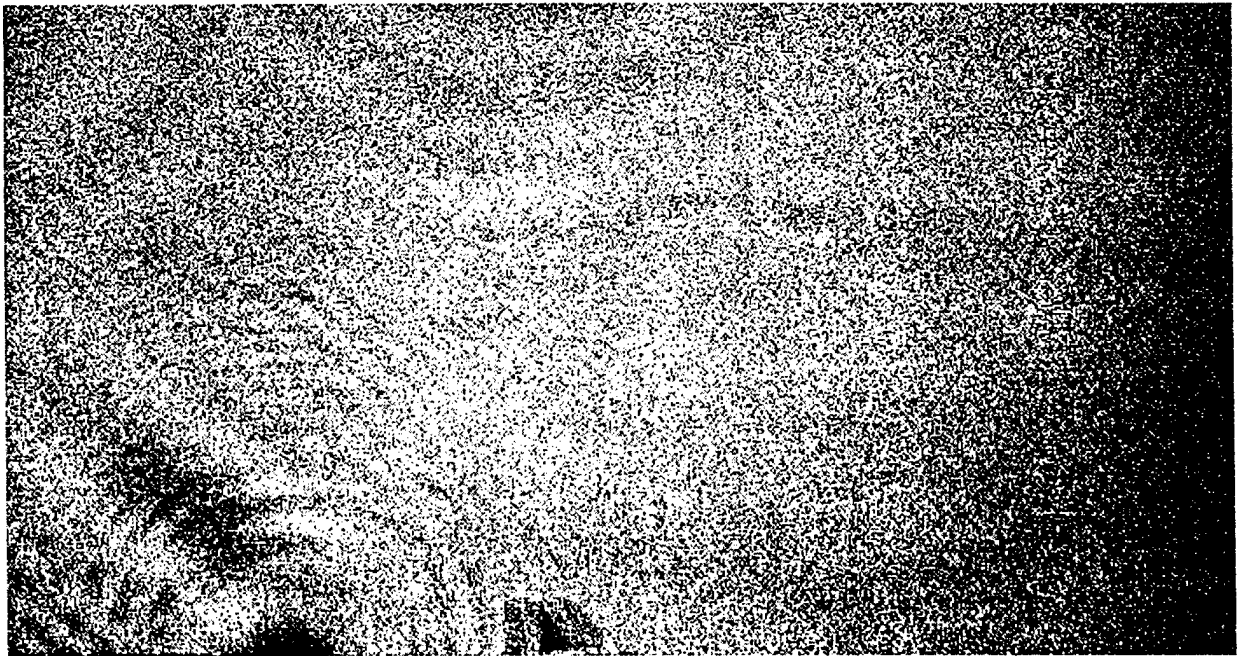
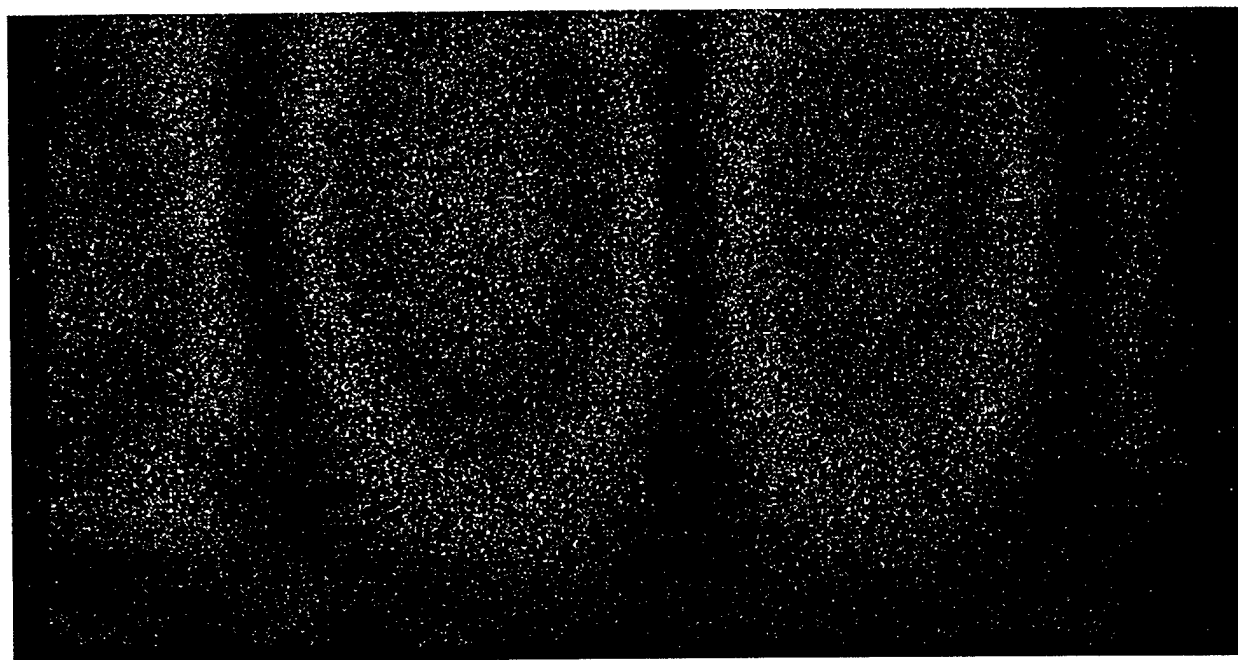
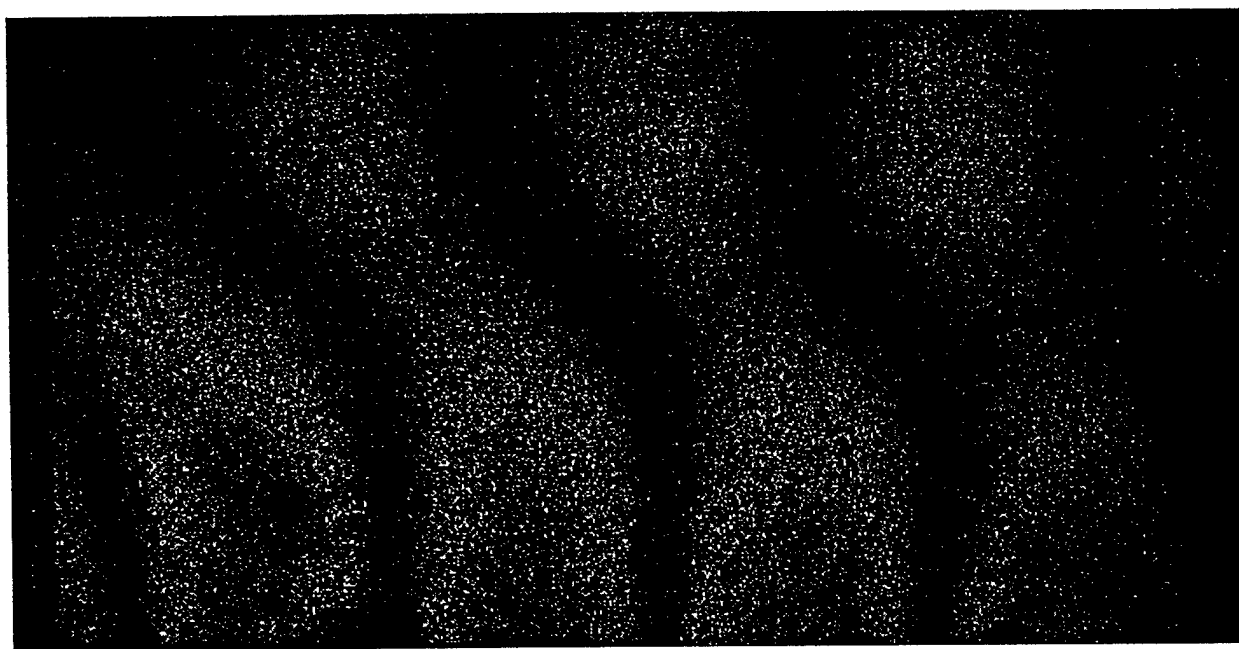


Figure 7. Shearograms of Panel #1

Panel #2 - 3rd Harmonic at 1650 Hz



Panel #2 - 4th Harmonic at 2900 Hz

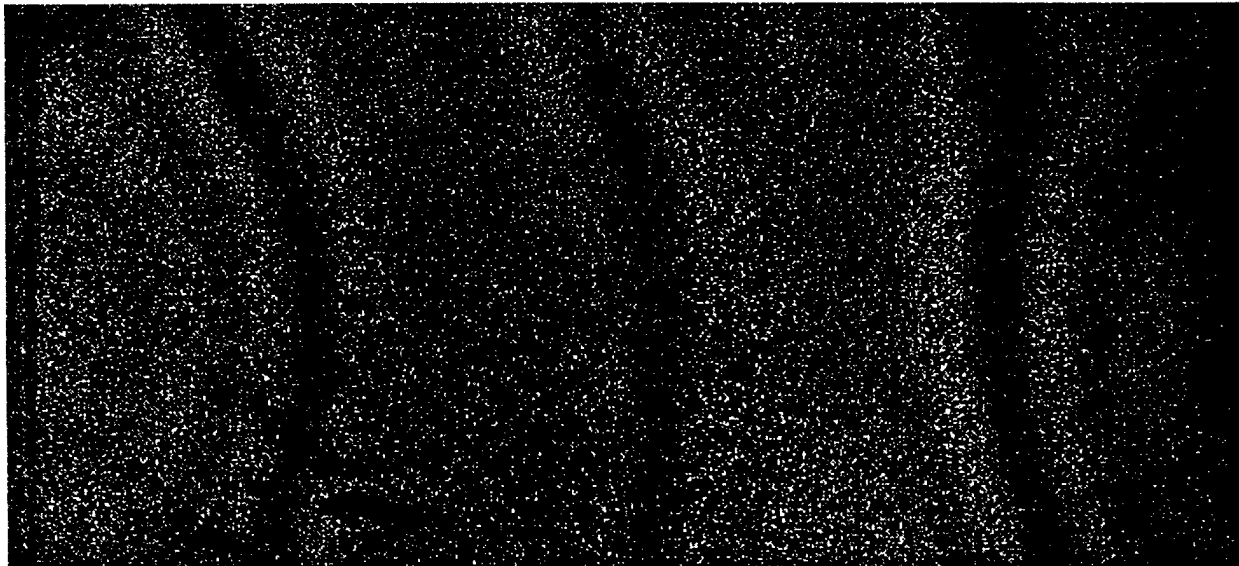


Reference Image Panel #2

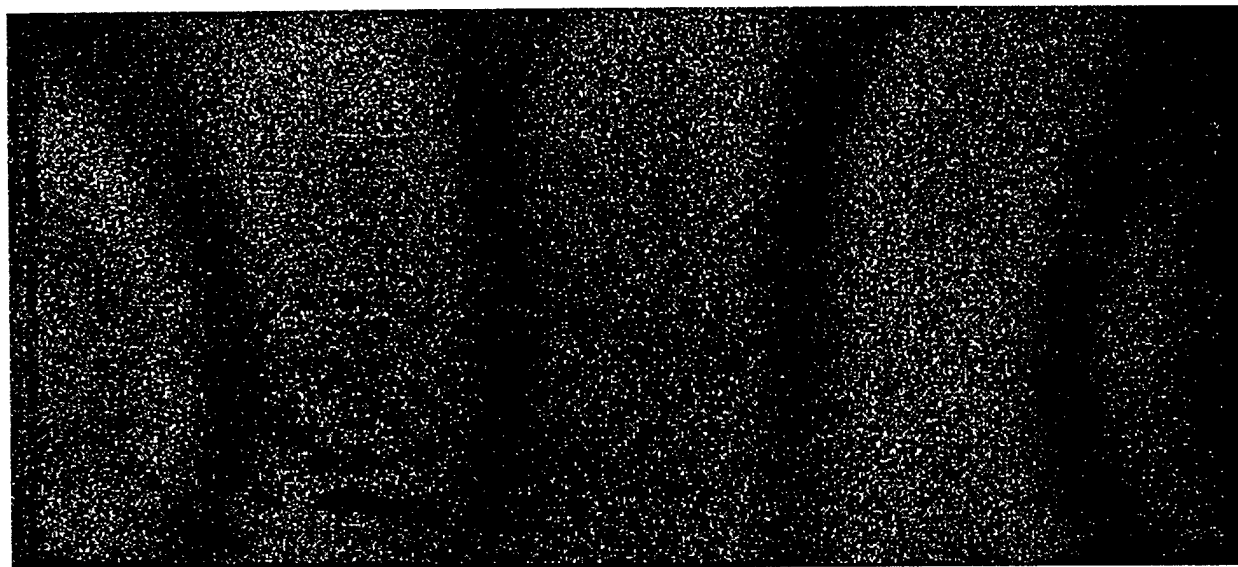


Figure 8. Shearograms of Panel #2

Panel #3 3rd Harmonic at 1600 Hz



Panel #3 4rd Harmonic at 2550 Hz



Panel #3 Reference Image

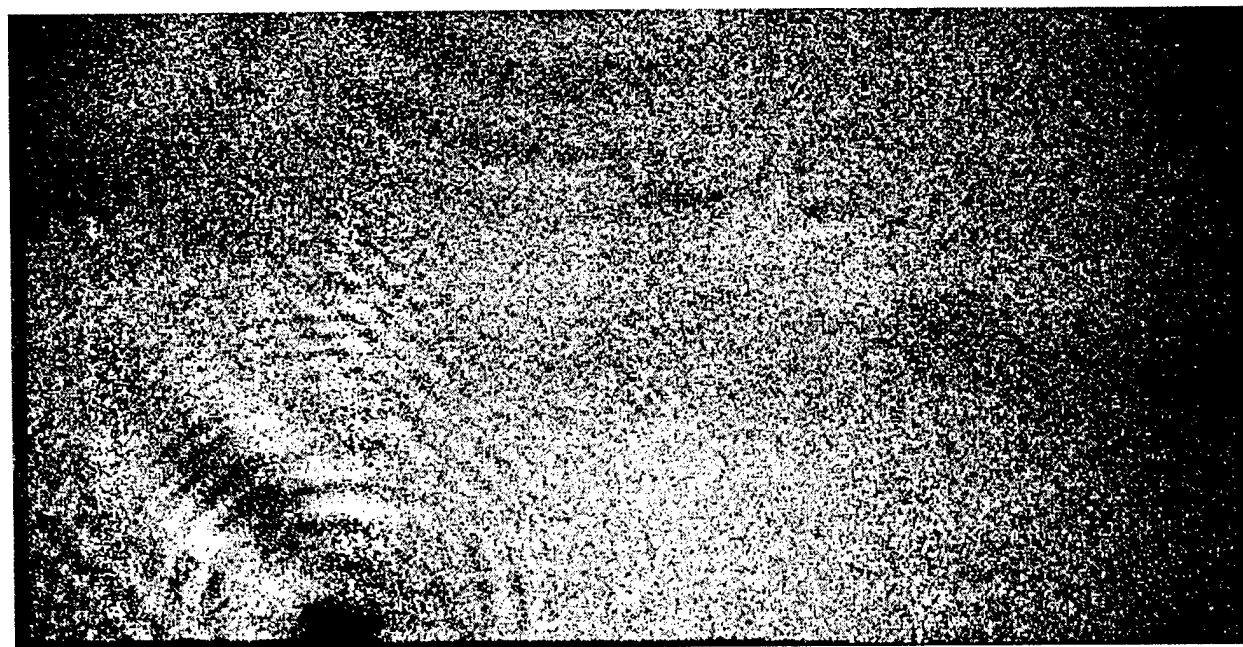


Figure 9. Shearograms of Panel #3

Panel #1 at the third harmonic exhibits almost vertical fringes and is easily discerned. At the 4th harmonic it is less well discerned but there are 4 broadly flat regions which indicate the 4 half wave sine waves.

Panel #2 also shows even more vertical fringes, but there is some rounding at the bottom of the panel which could indicate it is stiffer than it is in the middle. At the 4th harmonic the fringe pattern is only vertical for the first 50% and then angles off to the left. It is a symmetrical pattern.

Panel #3 shows no edge effects, but the fringes are not perfectly vertical. It is likely due to a small thickness variation along the panel in the Y axis.

The quantitative frequency data for 0.1045 inch thick modeled panels is presented below along with the laboratory obtained 3rd and 4th harmonics of bending.

Table 1. FEA and Lab Results for Test Panels at 3rd and 4th Harmonics

0.1045" thick	<u>FEA</u>	<u>FEA</u>	<u>FEA</u>	<u>Lab</u>	<u>Lab</u>	<u>Lab</u>
	Strong	Overall Weak	Checkerboard	#1	#2	#3
3rd Harmonic	1583 Hz	1320 Hz	1519 Hz	1700 Hz	1650 Hz	1600 Hz
4th Harmonic	2772 Hz	2050 Hz	2580 Hz	2800 Hz	2900 Hz	2550 Hz

The lab values at the third harmonic would indicate that panel #1 is the strongest as it vibrated at the highest frequency, #2 the 90% strength sample and #3 the 50% strength panel. However, the span between the strong panel and the 50% strong one is 100 Hz. The Q of the excitation resonance response was +/- 50 Hz for all samples; that is, varying the excitation frequency by 50 Hz did not fully destroy the resonance. For the 4th harmonic, panel #3 is still gauged as the weakest, but panel #2 is the strongest, and panel #1 would be the 90% strength specimen. It is interesting to note that for the 4th harmonic the percentage frequency difference between the weak and strong panel is $(2800-2550)/2800$ or 8.9%, while the difference at the third harmonic between the weak and strong panel is $(1700-1600)/1700$, or 5.9%. It appears exciting the panels at higher frequencies results in a greater sensitivity.

It is concluded quantitatively, that by gauging the results on the fourth harmonic, the order of strength from weakest to strongest is #3, #1 and #2. However, using the third harmonic as a gauging criterion, the order is #2, #3, and #1.

A coin drop test was also done where the panel is lightly wrapped with a rubber mallet. Each panel had a distinctive pitch. The results of listening to and ranking the pitch of each panel upon being struck are listed below.

Relative Ranking - Coin Drop Frequency Test Results

Panel #1 highest pitch
 Panel #2 same pitch as #1
 Panel #3 lowest pitch

This also leads to the conclusion that the relative panel strength went from 3 being the weakest, and either 1 or 2 the strongest.

The FEA results indicate the same trend. For the strong panel, concluded as #1 before the panel was destructively tested, the predicted frequency of the 3rd harmonic was 1583 versus 1700 Hz as measured

in the lab, again an approximately 100 Hz difference. And for the 4th harmonic it was in very close agreement; 2772 Hz. predicted versus 2800 Hz. measured. Finally, it is interesting to note that the lab results for panel #3 more closely agreed to the checkerboard weak model; 1600 Hz. versus 1519 Hz. at the 3rd harmonic, and 2550 Hz. versus 2580 Hz for the 4th harmonic. The checkerboard weak model was a normally bonded panel in only 50% of the area, the area being distributed randomly over the panel.

Destructive Testing

After shearography, the panels were sent back to Dr. Mantel for destructive testing. The panels were cut into 1 inch by 0.25 inch pieces and each piece was tested in three point cantilever until failure. The actual test is called the short beam shear test. Because there were approximately 240 small test pieces for the cantilever test, the results were averaged to one number. The short beam shear tests on the panels indicated that they did not break at the adhesive regardless of the assumed bond quality. A flatwise tensile test was then done and a difference was found. The results are that the panel #3 failed at an average strength of 3748.8 psi, panel #2 failed at 3998.2 psi and panel #1 failed at 2608.6 psi. The fabricated panels were to be normal, 10% and 50% strength, and instead had tested values of 93.7% and 65.2% of the strongest panel's strength. The following list details the destructive results.

<u>Panel ID#</u>	<u>Strength (psi)</u>	<u>std. dev (psi)</u>	<u>% Normal Strength</u>
#1 (WEAKEST)	2608.6	275.3	65.2%
#2 (STRONG)	3998.2	280.7	
#3 (MEDIUM)	3748.8	167.1	93.7%

It can be seen that #2 and #3 are quite close to the same strength although they were manufactured differently. Also, the panels were acoustically C-scanned before cutting into the small pieces for destructive testing. A statistical analysis of the pixel levels also showed that the difference between #2 and #3 is quite small.

Calibration

A unique instrument calibration technique was developed to gauge the absolute sensitivity of the shearing system. This technique can be applied to any shearing camera. Although it is a simple matter to get a fringe pattern from a shearing system for qualitative interpretations, it is more demanding to interpret a fringe pattern where the distance between the fringe lines can be regarded with a high degree of accuracy. The means developed to accomplish this was to present to the shearing camera a thin cantilever beam. The end of the beam was in contact with a differential micrometer. The micrometer tip was adjusted so that it was in slight contact with the end of the beam; this was the reference position. Then the tip was moved such that it bent the beam; this was the position to be calibrated. Using knowledge of how a beam behaves when deflected at its end, it is possible to arrive at a sensitivity factor for surface displacements between adjacent bright fringes. This method essentially determines the angle between the camera's viewing direction and the direction of the incident light. In most shearing systems there is a small angle between the viewing axis and the axis of the incoming illumination. The apparent wavelength of the laser is effectively changed by the multiplicative factor of the cosine of the angle between the viewing axis and the illumination axis. This calibration technique eliminates the

measurement of this angle and instead allows for the determination of overall scale factors by the measurement of fringes on an object of known shape.

A thin beam bent in cantilever with one end clamped and the other end free has a cubic shape:

Eqn. 4
$$y(x) = \frac{Fx^2}{6EI}(3l - x)$$

where:

F is the applied force at the end of the beam

x is the distance along the beam from the fixed end

l is the length of the beam

E is Young's modulus of the beam

I is the area moment of the beam, $wt^3/12$, where w is the width and t is the thickness

This equation is rewritten without regard to force and material properties to characterize its shape. Rewriting it in terms of the maximum deflection determined at $y(x=l) = y_{\max}$.

Eqn. 5
$$y_{\max} = \frac{Fl^3}{3EI} \text{ and}$$

Eqn. 6
$$\frac{y}{y_{\max}} = \frac{x^2(3l - x)}{2l^3} \text{ finally;}$$

Eqn. 7
$$y = \frac{y_{\max}}{2} \left(\frac{x}{l} \right)^2 \left(\frac{x}{l} - 3 \right)$$

The resulting shearogram of the beam will show one full fringe cycle for every $\lambda/2$ out of plane displacement of the beam; λ is the wavelength of the laser light. Since a shearogram is only sensitive to the slope of the surface, the resulting shearogram will reveal one full fringe every time the path length from the two points on the surface under test changes by half a wavelength. Mathematically this is expressed as:

Eqn. 8
$$\text{slope}(n) = n \lambda/s;$$

where n is the order and s is the shearing distance at the surface of the object.

The slope of this calibration beam as a function of distance is determined from the derivative of Eqn 7:

Eqn. 9
$$\frac{\partial y}{\partial x} = \frac{3y_{\max}}{2l^3} (2xl - x^2)$$

Setting the slope of the beam equal to the order of the slope sensitivity and solving for the fringe order yields:

Eqn. 10

$$n = \frac{3y_{\max}^s}{\lambda l^3} (2xl - x^2)$$

This technique produces an easy to implement "field" method of calibration of the entire shearing system; a shearogram is made of a beam and this reference image is stored. Then the end of the beam is deflected by a small amount and a second exposure is made. The two images are subtracted pixel by pixel on an intensity basis. By counting the number of fringes across the beam, the effective sensitivity of the system is determined without resorting to cumbersome physical measurements of the set up.

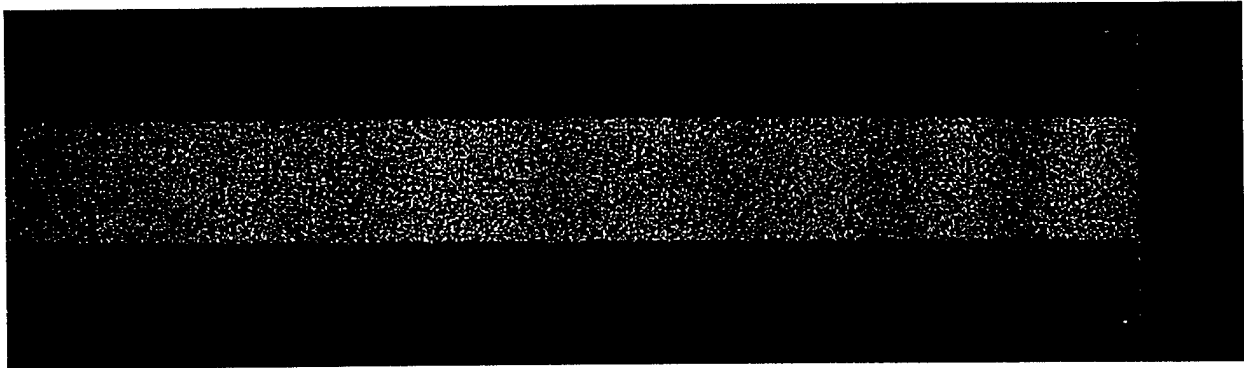


Figure 10 - Shearogram of Bent Cantilever Beam Calibration; tip deflection = 50 microns

Figure 10 is the shearogram made after deflecting the tip by 50 micrometers and subtracting the reference image. There was a total of 6 fringes visible from the fixed end to the deflected end; that is, $n = 6$. In the shearogram, the deflected tip is on the left and the fixed end of the beam is on the right. Note the fringe spacing is closer near the fixed end as Equation 9 indicates, and becomes more widely separated near the deflected end. For the shearing distance of 6.4 mm used in all the work, the slope sensitivity at the tip of the beam is determined to be 4.8×10^{-4} radians. In Figure 10, the measured distance between fringes 5 and 6 was 27 mm. The shearography apparatus has detected an out of plane height increase from fringe 5 to fringe 6 to be 13 microns.

Field System

Based on the results and experience obtained in the research, it is probably too labor intensive to create FEA models of every important portion of an aircraft. FEA simulations of the simple panels used in this work took days to calculate on a SUN workstation. This type of NDE testing requires that a predictive value be made before it is compared with field test values. This *a priori* requirement would make this type of testing extremely costly. It may be simpler to thoroughly test a new aircraft with shearography after it is first put into service. Then, over time, subsequent images would be compared to the frequencies at the same mode shapes. There is not a linear relationship between frequency of vibration and the strength left in the component. Image processing would be required to determine the "goodness

of fit" of the modal pattern of the aircraft with the stored reference modal pattern made early in its history.

CONCLUSIONS

A lab sheaogram system using acoustic excitation determined the highest strength of three composite panels whose strength was unknown to the experimenter prior to destructive testing. The observed frequency of excitation for a particular modal pattern also agreed well with the highest modal vibration frequency at the fourth bending harmonic of the panel with that predicted by FEA analysis. However, the lab system unfortunately misidentified the second strongest panel (#3, at 93.7% relative strength) as the weakest, and did so at both the third and fourth harmonics. One possible reason for this is that panels #2 and #3 were made using a slightly different process from panel #1.

Synchronous shearography is a much better optical NDE tool than holography because common mode movement does not blur the shearogram, and speckle noise is decorrelated. Acoustic excitation works best and is easy to implement. However, the extremely loud sound pressure levels, typically bordering on 125 dbA make the method unfriendly to nearby personnel. The sound does not last long, a few seconds is all that is necessary to "tune" in the modal pattern, but is nonetheless acutely loud. Microwave and passive thermal testing did not reliably yield shearograms which were interpretable. FEA work done on simple rectangular panels correlated well with laboratory results. The panels were acoustically excited at their 3rd and 4th harmonics and restricted to one axis of vibration, simulating panel flexure between ribs or stringers. The results agreed to within 4% of the FEA predicted values for excitation at the fourth harmonic.

The panels were fabricated in accordance with a Boeing specified process for producing carbon composite structural components capable of high temperature, high structural loads. The curing cycle used normal industry resins and Fiberite carbon fiber. Destructive testing after the lab tests determined the strength of the panels which agreed with the relative strengths as determined by the NDE method of shearography.

Based on the costs required to model an aircraft using FEA methods, it is not plausible to cost effectively create and store vibratory modal patterns of an aircraft's outer skin. Synchronous shearography may be very effectively used to determine weakening in the flexure strength of a structure section of an aircraft. Any weakening is denoted by a reduction in the acoustic excitation frequency required to produce the same modal pattern when the aircraft was first introduced into service. There was no linear relation found between strength and acoustic frequency due to the broad Q of the resonant modal patterns. The fact that one panel was made slightly differently than the others, likely masking this effect, is the likely cause. Excitation at slightly higher frequencies may prove more fruitful. Normal shearography uses frequencies whose longitudinal wavelengths (in the object under test) are on the order of the size of the local defect. For composites this frequency is in the range of 25 kHz to 30 kHz. For detecting overall weak structures, based on experience gained here, frequencies in the 4 kHz to 8 kHz range may prove more useful and sensitive.

Testing for an overall weak part is a much more difficult problem because the "signature" of a weak component is distributed over a large area and not restricted to an area the size of a coin. The signal is not really a pattern, but the observed reduction in the excitation frequency which produces the same modal pattern as was observed when the test object was verified as strong. A field system based on

lowered modal vibration frequency would have to be relatively insensitive when the object is tested at a later time. It would have to be able to automatically detect that the (substantially) same modal structure was present in the presence of to minor scale and alignment errors . High frequency shearography systems designed for finding small disbonds are available commercially. Their image processing is the same as described here, but it is tuned to look for the classic shearogram "butterfly" signal.